LOS Analysis for Localisation in High Frequency Systems

Ali Mahbas, *Member, IEEE,*, John Cosmas, *Senior Member, IEEE,*, Sarmad Mueen, *Member, IEEE,*, Jiangzhou Wang, *Fellow, IEEE,*

***Abstract*—The terahertz-wave communications are sensitive to the propagation environment. Line-of-Sight (LOS) is considered crucial in maintaining reliable connections between transmitters and receivers, providing high quality of service and estimating the terminals' locations accurately. Therefore, maximizing LOS availability improves performance and the localization process in the future systems. In this paper, we propose a general framework to investigate the impact of blockages' characteristics on the probability of a terminal of interest provided with a number of LOS links simultaneously by taking into consideration the correlation among these links. A comparison among three scenarios, namely correlation, no correlation and two-dimensional is presented to validate the accuracy of these scenarios in different environment densities. The simulation results validate the accuracy of our analysis and show that considering different values of the base station (BS) number and height can improve the system performance. Maximizing the LOS availability can be achieved by considering a higher number of BSs in low and medium environment densities and by increasing the height of BSs for dense environments. Furthermore, unlike in the low environment densities, the correlation between links needs to be addressed carefully when studying LOS availability in dense environments in order to meet the future requirements.**

***Index Terms*—Localisation, TDoA, AoA, LOS, blockage model, high frequency.**

I. Introduction

IN the context of 6G applications such as Internet of Things (IoT) and Industry 4.0, the localization process is critical and requires high accuracy of less than 1 centimetre. Time Difference of Arrival (TDoA) and Angle of Arrival (AOA) are considered as the main techniques for estimating locations [1]. However, the absence of Line-of-Sight (LOS) can result in misleading information and degrade the localization accuracy [2], [3]. In high frequency systems, such as Millimetre-wave (mmWave) and Terahertz-wave (THz-wave) systems, LOS availability has a significant impact not only on the localization process but also on establishing reliable connections to the receivers, in order to meet the various applications' requirements. This is because these systems face challenges such as penetration loss when passing through blockages like buildings.

It has been shown that the penetration loss on mmWave links caused by blockages (e.g. buildings) can reach up to 40 dB [4]–[6]. Therefore, investing the LOS opportunities in the system is crucial in these systems not only for evaluating the overall system performance, but also for a reliable localization system. In order to characterize the LOS availability in the system accurately the impacts of network density as well as correlation between links due to the blockages' densities, sizes and locations, need to be addressed carefully.

The correlation is defined as the dependency between the links due to the presence of blockages in the system [7], [19]. For instance, if there are two base stations (BSs) in the proximity of a user equipment (UE), the first BS (the closest BS to UE) becomes the serving BS when it provides LOS. However, when the first link is blocked by an object (e.g. building), the second BS can be the serving BS when it is not located in the same angle as the first BS (it is not blocked by the same object) and there is no other object blocking it. Because of the objects, both links become correlated (in other words, LOS availability of the further link is also dependent on the closer links). Note that this correlation is of less importance when the density of the environment is low [19]. However, the correlation between links becomes significant in dense environments. A higher environment density means shorter distances between the receiver and blockages. As a result the blocked area increases and the probability of blocking more links in the system increases. Furthermore, the sizes of the blockages can also impact the correlation. The correlation increases when the sizes of blockages increase. For example, when the UE is located very close to a large blockage (e.g. a large building), up to 50% of the scope will be blocked and as a result more links are likely to be blocked by the same blockage. Some papers made the assumption of no correlation between links in the system to simplify the analysis. Ignoring this impact in dense environments may cause misleading information. Therefore, we propose a new framework which considers a number of LOS links being available to the UE simultaneously in different environment densities by taking into account the correlation between links.

Due to the importance of LOS components for accurate and reliable localisation, some papers have addressed LOS and Non-LOS (NLOS) links in different wireless systems [8]–[12]. Two approaches have been used to identify both LOS and NLOS components in the localization process. In the first approach, different algorithms and solutions were proposed to identify and invest the available LOS components in the system. This is to minimize the inaccuracy due to NLOS components [8], [9]. In the second approach, both LOS and NLOS components were considered in the localization process [10], [11]. In [10], the location was estimated by using the Gaussian mixture model to model the errors in measurements.

In [11], a new method, robust weighted least squares, was used to formulate the localization problem given perfect identification of the LOS/NLOS measurements. Identifying the LOS components offers limited improvement to the localization process when the LOS availability in the system is limited.

Different from [8]–[12], other papers addressed and modelled the LOS availability in the terrestrial systems [13]–[22].

For sake of the mathematical derivation, a LOS ball model is an approach to characterize the LOS availability in the system [16]. The LOS ball model was studied in [15], [19]–[21]. [20] proposed a framework to model and investigate the coverage rate in a self-backhauld mmWave cellular network. It was assumed that any BS is LOS with a constant probability, if it is located within a specific area. This assumption partly ignores the distance-dependence, as all BSs are LOS with a constant probability. Although it is believed that the blockages' characteristics have a great impact on the LOS availability and on the mmWave system performance, [20] ignored the blockages' characteristics and their locations. The system performance in the small cell networks was studied in [15] by taking into account both LOS and NLOS components. It was assumed in [15] that the link to each BS is LOS with some probability and NLOS otherwise, where this probability is a function of the distance between the transmitters and the receiver of interest. This assumption is reasonable for low frequency systems, however, the mmWave and THz-wave systems are very sensitive to blockages and suffer from high propagation loss [6]. In [19], a framework is proposed to evaluate the coverage and rate performance in mmWave cellular networks. Using a distance-dependent LOS probability function, the locations of the LOS and NLOS BSs are modelled as two independent non-homogeneous Poisson Point Processes (PPP). In [21], a stochastic approximation to system analysis of a cellular network was proposed where the practical aspects, such as LOS and NLOS propagation, and general fading channels, were considered. The blockages' characteristics were ignored, however, the probability of any link being LOS does not only depend on the distance but also on the blockages' characteristics and locations as will be shown in this paper. Another drawback of the LOS ball model [15], [19]–[21] is that the links to different BSs are assumed to be independent of each other (no correlation between links). The random shape theory is another approach to address the LOS availability [17], [18]. In [17], the random shape theory was used to model the blockages' characteristics such as the locations and dimensions. Similar to other papers [15], [20], one of the main drawbacks in this work is that the correlation among links was not considered. This assumption can affect the analysis in a dense environment significantly as explained earlier in this paper. [18] proposed an analytical framework to define and characterise the connectivity for an aerial access point by jointly using stochastic geometry and random shape theory. The buildings are modelled as a Boolean line-segment process with fixed heights. [18] used the same approach as in [17]. In [13], the probability of link to the receiver being LOS is studied by using the line Boolean model for modelling the blockages in the system. Although this paper considered the correlation between links due to the size and density of blockages, the work ignored the blockages' characteristics. For instance, this work assumes that the link is blocked and tagged as a NLOS, if a blockage falls on the link between UE and the anchor (note that the anchor and BS are used interchangeably throughout this paper). This can happen if the heights of blockages are greater than the height of anchors. However, in reality the heights of blockages can be shorter than the height of anchors. As a result, the link sometimes can be unblocked even if the blockages are located between the transmitters and receivers as will be shown further below in our paper. The other drawback of this paper is that the lines may overlap due to the nature of PPP which was used for modelling the blockages in a dense environment. In reality the blockages (e.g building) can not overlap. In [14], the signal to interference and noise ratio (SINR) coverage probability is derived by considering the correlation between the blockages and, serving and interference links. Similar to [13], this work also assumes that blockages are distributed as a PPP. The other drawback of the aforementioned papers is that the BSs are distributed as a PPP and the distance to the serving cell is unrestricted. This assumption is acceptable in low frequency systems, however, it is not valid in the high frequency systems due to the high propagation loss and the communication links not being able more than a few hundreds meters in mmWave and THz-wave systems [5], [23]. In [22], the localisation is addressed by using stochastic geometry. The probability of having a sufficient number of LOS anchors is studied. For sake of simplification, this paper only considered the correlation between the first and the second blockages in the environment. Similar to [13], this paper considered a two-dimensional environment in which the heights of UE, anchors and blockages are ignored.

The LOS availability has also received significant attention in the unmanned aerial vehicle (UAV) communications. Recent papers have addressed different aspects of mmWave UAV systems such as coverage analysis, uplink performance analysis, downlink performance analysis, path planning and power control [27]–[35]. It is believed that addressing the probability of LOS is of vital importance to support the emerging bandwidth-hungry applications facilitated by UAVs operating in mmWave frequency bands. Most of the recent papers, including the aforementioned ones, considered the probability of LOS model presented in [36]. This model is an overly optimistic approximation and its applicability is limited due to the assumption made that the blockages (e.g. buildings) bases are perpendicular to the LOS projection between the transmitter and the receiver [27]. In [27], a LOS probability model in UAV communication setups over regular urban grid deployments, which is based on a Manhattan Poisson line process, where the blockages' characteristics are taken into account. It is anticipated that the LOS availability in the mmWave systems can be provided by multiple BSs in the proximity of the UE. This paper derived the LOS availability to one BS, which means other LOS opportunities in the system are not captured in the model proposed. The other limitation in the aforementioned UAV studies is that the dependency between links are not considered. It is believed that the probability of LOS in the UAV communications requires an air-to-ground model, which is different from the probability

of LOS in the terrestrial communications [35]. Studying the LOS availability in the UAV communications is considered as a future work.

The main difference between the aforementioned papers and our work is that the probability of an anchor being LOS is a function of, not only the distance to UE, but also the blockages' locations and characteristics (e.g. heights). Furthermore, the correlation between links is considered when studying the LOS availability to each anchor. In this work we also model the probability of a number of links being LOS simultaneously which is crucial for estimating UEs locations accurately. Our work presents a framework to study the impacts of different system parameters and environment characteristics on the availability of LOS links in the system, which is of vital importance in the system design to boost the LOS availability and improve the localization process.
The contribution is summarized as follows:

- The locations of blockages and BSs are modelled by using stochastic geometry, where the hard core point process (HCPP) is used to model the locations of different types of blockages, while the binomial point process (BPP) is used to model the locations of BSs in the system. In order to study the probability of a link being LOS, the blockages located on the straight line between a reference UE and any BS in the area are mapped into a one-dimensional marked point process (MPP).
- We propose a novel framework in which the LOS probability is derived by taking into consideration different environment parameters (blockage's dimensions, density and locations) and network parameters (e.g. number, height and locations of BSs). Furthermore, the correlation between links is also considered, in order to minimize the misleading information when addressing different environment densities.
- The probability of each BS providing LOS to the reference UE is derived by using the proposed framework. This probability is a function of distances to the blockages and BSs in the system as well as the blockage characteristics and BSs heights.
- The proposed framework can also support other aspects of the wireless communication systems such as localization. The probability of at least N_L BSs being LOS simultaneously is derived for three scenarios: i) correlation ii) no correlation iii) two-dimensional. This is to compare and validate the main approaches and assumptions in literature. Furthermore, several special cases are considered and investigated for their practical importance, such as N_L = 1 for maintaining a reliable connection in high frequency systems, N_L = 2 for estimating the UE location by using AOA and, N_L = 3 for estimating UE's location in 2D and N_L = 4 for estimating UE's location in 3D by using TDoA.
- This paper further demonstrates a performance comparison between our analysis (where the correlation among links is considered) and the analysis under assumption of no correlation between links. Furthermore, the impact of different parameters such as density, dimensions and locations of blockages, and the number and height of BSs in the area is also captured.

The rest of this paper is structured as follows: Section II describes the system model. The probability of Line-of-Sight is investigated in Section III. In Section IV, the system performance is shown by simulation results. Conclusions are drawn in Section V.

II. System Model

Consider a cellular network as shown in Figure 1. It is assumed that the system contains BSs with height h_b and N_g types of blockages (e.g. different sized buildings, trees). It is also assumed that a blockage of ith type has a regular shape and is described by the triple $\{(w_i, l_i, h_i)\}$, where w_i, l_i and h_i are the width, the length and the height of ith blockage respectively. Before, we propose a framework to model the probability of a reference UE ($\mathcal{U}_0$) provided with N_L LOS links simultaneously, the blockages need to be investigated in the system. Next, we make some assumptions to clarify the system model and the locations of blockages in the system.

Assumption I: It is assumed that the link (mmWave and THz-wave) can only be established between $\mathcal{U}_0$ and any BS when the distance between them is less than R_{mm}. This assumption is consistent with the measurements carried out by [5] and some studies [23], where a link can only be established within a tens of meters distance.

Assumption II: It is assumed that the BSs with height of h_b are distributed as binomial point process (BPP) in the system. BPP is a more accurate model when studying a finite network [24], [25].
From Assumption I and Assumption II, $\mathcal{U}_0$ is assumed to be at the centre of a circle of R_{mm} radius. Furthermore, $\mathcal{U}_0$ can only be associated with the N_b BSs located in the area $R_{mm}^2\pi$.

Assumption III: Modelling the blockages by using one of the random point processes has been accepted in the mmWave systems [17]. In this paper, it is assumed that the centres of blockages in the system are modelled as a Hard Core Point Process (HCPP) [26]. Unlike PPP, HCPP doesn't allow any two points to be closer than a minimum distance. This process is considered more suitable to model the locations of blockages (e.g. trees and buildings). HCPP is used to ensure that the blockages are not overlapped.

From Assumption III, the centres of blockages in the system are modelled as a HCPP. The parent process of the blockages can be expressed as marked point process (MPP) $\Phi_p = \{(y_j, \tau_{y_j}), \theta_{y_j}, i\}_{j\in\Phi_p}$ with density λ_p, where y_j represents the location of jth point, τ_{y_j} is a mark attached to each point in the process and uniformly distributed in the range $[0, 1]$, θ_{y_j} represents the orientation angle of jth point and is uniformly distributed in the range $[0, 2\pi]$, and i represents the blockage type and takes a value in the range $[1, 2, \cdots, N_g]$. The jth point is associated with the mark i with probability of ρ_i where $i \in [1, 2, \cdots, N_g]$ and, ρ_i takes a value between 1 and 0 and $\sum_{i=1}^{N_g} \rho_i = 1$. The density of blockages in the system can be obtained as follows.

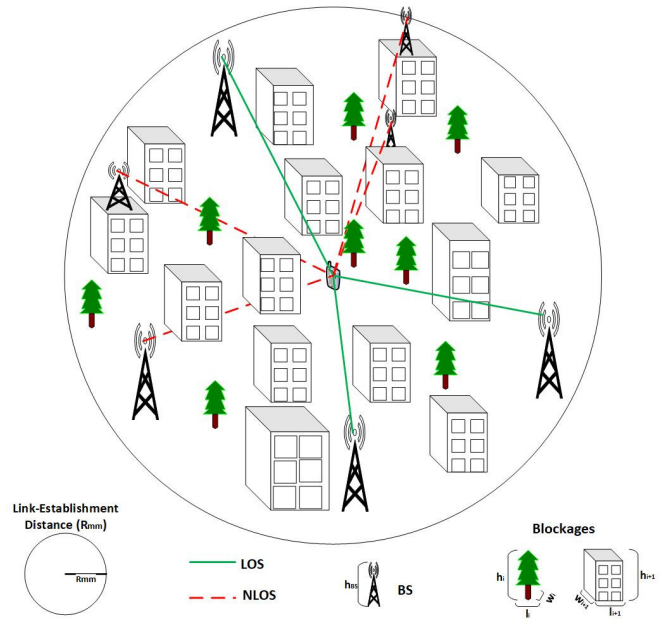

Fig. 1. System Model.

Lemma 1 The total density of the blockages in the environment can be obtained as:

$$\lambda_o = \lambda_p \sum_{i=1}^{N_g} \rho_i \mathcal{P}_{o,i} \tag{1}$$

where $\mathcal{P}_{o,i} = \prod_{n=1}^{N_g} \frac{1-e^{-\lambda_p \rho_n \pi r_{i,n}^2}}{\lambda_p \rho_n \pi r_{i,n}^2}$ represents the probability of a point of ith type being retained, and $r_{i,n}$ represents the exclusion distance of the point from ith type and a point from nth type.

Proof: The blockages in the system is modelled by using HCPP. The new process Φ_o with density λ_o will be also random but non-homogounius [26]. The jth point with the mark τ_{y_j} from the ith type is retained, if $\tau_{y_j,i} < \min \tau_{y_q,n}, y_q \in (\mathcal{D}_{y_j,i}(r_{i,n}) \bigcap \Phi \backslash y_j)$, where $\mathcal{D}_{y_j,i}(r_{i,n})$ represents a disc of radius $r_{i,n}$ centred at the point y_j. $r_{i,n}$ is a random variable and depends on the orientation angles θ_{y_j} and θ_{y_q}. Since the orientation angle is independent of the locations of the points, $r_{i,n}$ is assumed to be uniformly distributed in the range $[(w_i/2 + w_n/2), (\sqrt{\frac{w_i^2}{4} + \frac{l_i^2}{4}} + \sqrt{\frac{w_n^2}{4} + \frac{l_n^2}{4}})]$. When the number of nth type points is located in $\mathcal{D}_{y_j}(r_{i,n})$ is η_n, the probability that τ_{y_j} has the minimum value is $\prod_{n=1}^{N_g} \frac{1}{\eta_n+1}$ where $\eta_n > 1$. The probability of a random point of the ith type being retained can be obtained as:

$$\begin{aligned} \mathcal{P}_{o,i} &= \prod_{n=1}^{N_g} \sum_{\eta_n=0}^{\infty} \mathbb{P}\Big((\mathcal{D}_{y_j}(r_{i,n} \bigcap \Phi \backslash y_j) = \eta_n \Big) \\ &= \prod_{n=1}^{N_g} \sum_{\eta_n=0}^{\infty} \frac{e^{-\lambda_p \rho_n \pi r_{i,n}^2} (\lambda_p \rho_n \pi r_{i,n}^2)^{\eta_n+1}}{(\eta_n+1)!} \\ &= \prod_{n=1}^{N_g} \frac{1 - e^{-\lambda_p \rho_n \pi r_{i,n}^2}}{\lambda_p \rho_n \pi r_{i,n}^2} \end{aligned} \tag{2}$$

The total density of ith blockage can be obtained as $\lambda_{o,i} = \lambda_p \mathcal{P}_{o,i} \rho_i$. The final result in Eq. (1) is reached after summing up all densities of blockages in the system. ■

Since BSs are randomly distributed in the system and independent of the blockages process Φ_o, some of the BSs will be located where some of the blockages (e.g. buildings) are. Therefore, it is considered that any BS located on a blockage is installed on the roof or on the side of that blockage. In this paper, it is also assumed that $\mathcal{U}_0$ is located uniformly in the system and it is not part of the blockages process. Without loss of generality, $\mathcal{U}_0$ is located at the origin, thus the probability of $\mathcal{U}_0$ being outdoor can be obtained in the next Lemma.

Lemma 2: The probability of $\mathcal{U}_0$ being outdoor can be expressed as

$$\mathcal{P}_{Out} = \exp\Big(-\pi \sum_{i=1}^{N_g} \lambda_{o,i} r_i^2 \Big) \tag{3}$$

Proof: Since the location of $\mathcal{U}_0$ is not part of the blockage process, $\mathcal{U}_0$ is considered indoor if the distance between $\mathcal{U}_0$ and the centre of blockage from ith type is shorter than r_i. Assuming that $N_g = 1$ and χ represents the distance between $\mathcal{U}_0$ and the nearest blockage, the probability of $\mathcal{U}_0$ located indoor can be found as

$$\begin{aligned} \mathcal{P}_{In} &= 1 - \mathbb{P}\big[\chi > r\big] \\ &= 1 - \exp\Big(-\pi \lambda_o r^2 \Big) \end{aligned} \tag{4}$$

the above equation shows that $\mathcal{U}_0$ is considered indoor if it is located at distance r or less from the centre of the blockage. r is uniformly distributed in the range $[w_i, \sqrt{\frac{w^2}{4} + \frac{l^2}{4}}]$, and $\mathbb{P}\big[\chi > r\big]$ is the probability of $\mathcal{U}_0$ located at the origin and being at a distance greater than r from the nearest blockage (it is found from null probability) [26]. The probability of $\mathcal{U}_0$ being outdoor can be found

$$\mathcal{P}_{Out} = 1 - \mathcal{P}_{In} \tag{5}$$

When there are N_g types of blockages in the system, the probability of $\mathcal{U}_0$ being indoor can be found

$$\begin{aligned} \mathcal{P}_{In} &= 1 - \prod_{i=1}^{N_g} \mathbb{P}\big[\chi_i > r_i\big] \\ &= 1 - \exp\Big(-\pi \sum_{i=1}^{N_g} \lambda_{o,i} r_i^2 \Big) \end{aligned} \tag{6}$$

The results in (3) is reached. ■

Since the blockages are at different distances from $\mathcal{U}_0$ and located between BSs and $\mathcal{U}_0$, some of these blockages block the LOS to BSs. For instance, when $h_i > h_b$, any blockage of ith type will always block the LOS to kth BS as long as the blockage is located on the straight line between $\mathcal{U}_0$ and kth BS. When $h_b > h_i$, any blockage of ith type will only block the LOS between $\mathcal{U}_0$ and kth BS if this blockage is placed on the straight line at the blocking distance ($\mathbb{B}_{k,i}$) or less as shown in Fig 2. The blocking distance can be obtained as:

$$\mathbb{B}_{k,i} = R_k \Psi_i \tag{7}$$

where R_k is the distance between $\mathcal{U}_0$ and kth BS, $\Psi_i = \frac{h_i - h_u}{h_b - h_u}$ and h_u is the height of $\mathcal{U}_0$. When h_i takes a value equals or greater than h_b, $\Psi_i \geq 1$. This means that any blockage will

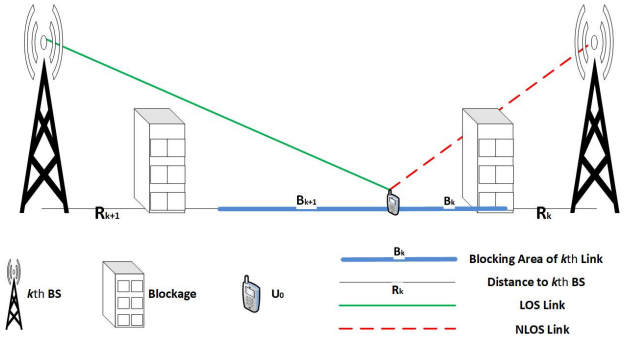

Fig. 2. Blocking Distance.

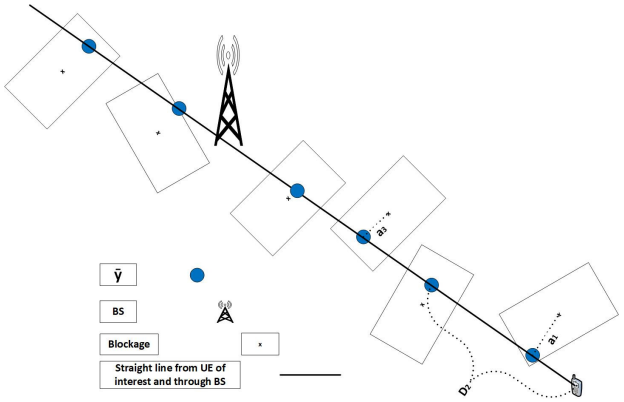

Fig. 3. Mapping Process.

block the LOS if it is located on the straight line between $\mathcal{U}_0$ and kth BS.

In order to establish whether any BS providing LOS to $\mathcal{U}_0$ or not, the impact of blockages due to locations and dimensions need to be investigated. Studying such system is considered challenging and most of studies tickling this issue made significant assumptions to simplify the analysis (e.g. no correlation and ignoring the blockages' characteristics). However, making such assumptions may compromise the accuracy as explained in Introduction section of this paper. Thanks to the random point process's tractability and flexibility, the blockages process can be mapped into more tractable process without any compromise on accuracy as shown latter in this paper. We map the blockages located on the straight line between $\mathcal{U}_0$ and kth BS into one dimensional MPP. Note that mapping in the next Theorem is crucial in our analysis.

Theorem 1 If $\mathcal{L}_k$ represents the straight line starting at $\mathcal{U}_0$ and passing through the location of kth BS, the blockages located on $\mathcal{L}_k$ can be mapped into one dimensional MPP on $\mathbb{R}^+ \times [0, z_i]$:

$$\bar{\Phi}_k = \{(\bar{y}_m, a_m), i\} \tag{8}$$

of intensity:

$$\bar{\lambda}_k = \sum_{i=1}^{N_g} 2 z_i \rho_i \prod_{n=1}^{N_g} \frac{1 - e^{-\lambda_p \rho_n \pi r_{i,n}^2}}{\rho_n \pi r_{i,n}^2} \tag{9}$$

where $\bar{y}_m$ is the closest point to the centre of mth blockage and located on $\mathcal{L}_k$, i represents the blockage type and takes a value in the range $[1, 2, \cdots, N_g]$, and a_m represents the vertical distance between $\bar{y}_m$ and the centre of mth blockage. a_m is randomly distributed in the range $[0, z_i]$.

Proof: Assume that the number of blockages equals to one ($N_g = 1$) and number of BSs in the area of interest equals to one ($N_b = 1$). Some of the blockages are located on $\mathcal{L}$ and the centres of these blockages will be at distances in the range $[0, z]$ from $\mathcal{L}$. We refer to the closest points on $\mathcal{L}$ to the centres of these blockages as CPs. The locations of CPs on $\mathcal{L}$ are represented by $\bar{y}$ as shown in Fig. 3. Since the blockages are randomly located around $\mathcal{L}$, the distance between the centre of mth blockage and $\bar{y}_m$ is represented by a_m where $a_m \leq z$.

We map the blockages located on $\mathcal{L}$ into one dimensional MPP as shown:

$$\bar{\Phi} = \{(\bar{y}_m, a_m)\} \tag{10}$$

Since blockages located on $\mathcal{L}$ are randomly distributed in the area around $\mathcal{L}$, it is assumed that a_m is uniformly distributed in the range $[0, z]$ and $\bar{y}$ (the locations of CPs) are randomly distributed on $\mathcal{L}$ as one dimensional PPP. Note that the centres of blockages crossing $\mathcal{L}$ are located in the area surrounding $\mathcal{L}$ ($2zR$). The number of blockages centres in the area $2zR$ is represented by $\bar{N}$. It is assumed that the number of CPs on $\mathcal{L}$ for the R distance is represented by $\bar{N}_{CP}$. Since each CP represents one blockage located on $\mathcal{L}$, $\bar{N}_{CP} = \bar{N}$. The density of one dimensional MPP can be expressed as:

$$\begin{aligned} \bar{N} &= \bar{N}_{CP} \\ 2zR\lambda_o &= R\bar{\lambda} \\ \bar{\lambda} &= \frac{2z(1 - e^{-\lambda_p \pi x^2})}{\pi x^2} \end{aligned} \tag{11}$$

where λ_o is the density of blockages in the system and obtained in Eq. (1) when $N_g = 1$. Since CPs are randomly distributed as PPP on $\mathcal{L}$, the expected distance between $\mathcal{U}_0$ and the mth CP can be expressed as:

$$\mathbb{E}[D_m] = \int_0^\infty \mathrm{d}\, f_d(\mathrm{d}) d\mathrm{d} \tag{12}$$

D_m for $i > 0$ has an Erlang or Gamma distribution with m and $\bar{\lambda}$, therefore $f_d(\mathrm{d})$ is

$$f_d(\mathrm{d}) = \begin{cases} \frac{\bar{\lambda}_{o,k}^m}{\Gamma(m)} \mathrm{d}^{m-1} e^{-\bar{\lambda}_{o,k}\mathrm{d}}, & \mathrm{d} > 0 \\ 0, & \text{otherwise} \end{cases} \tag{13}$$

When the number of BSs is greater than one ($N_b > 1$) and the number of blockage types is greater than one in the system ($N_g > 1$), $\bar{y}_m$ is from ith type with probability of $\rho_i \prod_{n=1}^{N_g} \frac{1 - e^{-\lambda_p \rho_n \pi r_{i,n}^2}}{\rho_n \pi r_{i,n}^2}$ as shown in Lemma 1. $\bar{y}_m$ is at distance of a_m from the centre of mth blockage from ith type where a_m is randomly distributed in the range $[0, z_i]$. The result in (9) is reached after summing up all the densities of different blockage types. ■

Comments on Theorem 1

- Studying the distribution of blockages around the straight line between $\mathcal{U}_0$ and any BS is essential to estimate the LOS availability in the system. For sake of simplicity, the process of blockages distribution is mapped into a number of one-dimensional MPP.

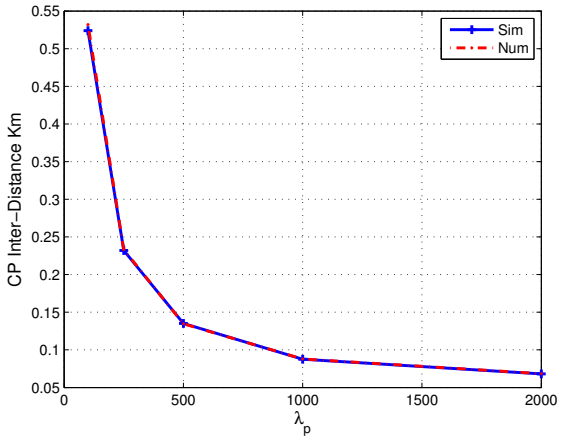

Fig. 4. Num is obtained by using Eq. (12) and Sim represents simulations.

- The mapping is accurate. Fig. 4 confirms the analysis with no compromise on analysis accuracy.
- The simulation results (Sim) in Fig. 4 are obtained from i) modelling blockages' locations by using HCPP as explained in Assumption III, ii) modelling the BSs' locations by using BPP as explained in Assumption II, iii) specifying the blockages located on $\mathcal{L}$, iv) locating CPs and measuring the inter-distance v) comparing the results of inter-distance to Num which is obtained by using Eq. (12).
- The above mapping produces a number of independent processes. However, the straight lines between $\mathcal{U}_0$ and any two BSs are correlated as one blockage can be located on one straight line or more. As a result, one blockage can block the LOS to one BS or more. The correlation among these processes are captured in the next section.

III. Probability of Line-of-Sight

In the localization process (e.g. Lateration), a number of simultaneous LOS BSs are required to estimate the UE's location precisely. For instance, four BSs (anchors) are required to estimate the UE's location when using TDOA. In this section, the probability of at least N_L simultaneous LOS links being available to $\mathcal{U}_0$ is derived in three scenarios, i) uncorrelated links, ii) correlated links and iii) two-dimensional environment. The main difference between the correlated links and uncorrelated links scenarios that in the latter it assumes that the links are independent and the correlation between these links is ignored. In the correlated links scenario, the dependency between links is captured. Furthermore, in the two-dimensional environment, the heights of blockages, $\mathcal{U}_0$ and BSs are not considered in the analysis. When there are N_b BSs in the area and the minimum number of simultaneous LOS links required for localization is N_L ($N_b \geq N_L$), it will be N_s possible sets of BSs to perform the localization. For instance, if the number of BSs in the area is 4 ($N_b = 4$) and the number of BSs required for performing localization is 3 ($N_L = 3$), there will be 4 possible sets of BSs $N_s = 4$ (S_{123}, S_{124}, S_{134} and S_{234}) where S_{123} represents the set of the first, second and third BSs, while S_{234} represents the set of the second, third and fourth (last) BSs. Note that the first BS is the closest BS to $\mathcal{U}_0$ and N_s can be obtained from:

$$N_s = \frac{N_b!}{N_L!(N_b - N_L)!} \tag{14}$$

The probability of at least N_L simultaneous LOS links being available to $\mathcal{U}_0$ is obtained from:

$$\mathbb{P}_{N_b,N_L} = \sum_{j=1}^{N_b-N_L+1} \sum_{k=j+1}^{N_b-N_L+2} \cdots\cdots \sum_{m=.+1}^{N_b-1} \sum_{n=m+1}^{N_b} \mathcal{S}_{jk\cdots mn} \tag{15}$$

where $\mathcal{S}_{jk\cdots mn}$ is the probability of at least N_L BSs (jth, kth, mth and nth BSs) of the $S_{jk\cdots mn}$ set being LOS simultaneously. In the next subsections, we consider a few cases due to practical importance. For instance, $N_L = 1$ means that there is at least one BS being LOS to $\mathcal{U}_0$. This is very important for maintaining a reliable connection in high frequency systems (THz-wave and mmWave systems). $N_L = 2$, $N_L = 3$ and $N_L = 4$ are considered very important for some of the localization methods. For instance, AoA requires at least two anchors while TDoA requires at least three anchors for 2D localization and four anchors for 3D localization [1].

A. No Correlation

The uncorrelated links scenario is considered in this subsection. Before deriving the probability of LOS for number of links in the system, first we study the probability of a BS being LOS in the next Lemma. The probability of kth link being LOS is obtained in the next Lemma.

Lemma 3 The probability of kth BS being LOS or unblocked by any blockage $\mathfrak{s}_k$ can be expressed as:

$$\mathfrak{s}_k = \sum_{i=1}^{N_g} \int_0^{R_{mm}} \exp\Big(-\omega_{k,i}\Big) f_{R_k}(r) dR_k \tag{16}$$

where $\omega_{k,i} = \bar{\lambda}_k \rho_i (R_k \Psi_i + \sqrt{x_i^2 - a_m^2})$, $f_{R_k}(r) = \frac{1}{R_{mm}} \beta(\frac{r}{R_{mm}}; k, N_b - k + 1)$ represents the property density function (PDF) of random variable R_k, $\bar{\lambda}_k \rho_i$ represents the density of ith CPs type on $\mathcal{L}_k$, $\beta(c; a, b)$ represents the beta density function defined as $1/B(a,b)c^{a-1}(1-c)^{b-1}$ and $B(.)$ is the beta function.

Proof: Assume that there is one blockage type in the system $N_g = 1$. The link to kth BS is considered LOS, if there is no blockage located on $\mathcal{L}_k$ at distance ω_k or shorter. In other words, the link is considered LOS if the first CP $\bar{y}_1$ is located at distance greater than ($\omega_k = R_k \Psi + \sqrt{x^2 - a_m^2}$). Since the CPs ($\bar{y}$) are distributed on $\mathcal{L}_k$ as PPP as shown in **Theorem 1**, the probability of no $\bar{y}$ located at distance (ω_k) or less is expressed as:

$$\begin{aligned} \mathfrak{s}_k &= \mathbb{P}[\text{No blockage at shorter distance than } \quad (\omega_k)] \\ &= \mathbb{P}[D > \omega_k] \\ &= \exp\Big(-\bar{\lambda}_k \omega_k\Big) \end{aligned} \tag{17}$$

where D represents the minimum distance between $\mathcal{U}_0$ and the nearest $\bar{y}$. Since the BSs are distributed as BPP in the system, the PDF of R_k is obtained in [24]:

$$f_{R_k}(r) = \frac{1}{R_{mm}} \beta(\frac{r}{R_{mm}}; k, N_b - k + 1) \tag{18}$$

where $\beta(c;a,b)$ represents the beta density function defined as $1/B(a,b)c^{a-1}(1-c)^{b-1}$ and $B(.)$ is the beta function. If $N_b = 6$, $\mathfrak{s}_k$ is obtained:

$$\mathfrak{s}_1 = \frac{E_0 - 5E_1 + 10E_2 - 10E_3 + 5E_4 - E_5}{R_{mm}B(1,6)}$$
$$\mathfrak{s}_2 = \frac{E_1 - 4E_2 + 6E_3 - 4E_4 + E_5}{R_{mm}B(2,5)},\ \mathfrak{s}_3 = \frac{E_2 - 3E_3 + 3E_4 - E_5}{R_{mm}B(3,4)}$$
$$\mathfrak{s}_4 = \frac{E_3 - 2E_4 + E_5}{R_{mm}B(4,3)},\ \mathfrak{s}_5 = \frac{E_4 - E_5}{R_{mm}B(5,2)},\ \mathfrak{s}_6 = \frac{E_5}{R_{mm}B(6,1)} \tag{19}$$

where $E_0, E_1, E_2, E_3, E_4, E_5$ are:

$$E_0 = \frac{1 - e^{-\psi R_{mm}}}{\psi}, \qquad E_1 = \frac{(1 - e^{-\psi R_{mm}}(R_{mm}\psi + 1))}{R_{mm}\psi^2}$$
$$E_2 = \frac{\hat{E}_2}{R_{mm}^2\psi^3},\ E_3 = \frac{\hat{E}_3}{R_{mm}^3\psi^4},\ E_4 = \frac{\hat{E}_4}{R_{mm}^4\psi^5},\ E_5 = \frac{\hat{E}_5}{R_{mm}^5\psi^6} \tag{20}$$

where $\hat{E}_2 = (e^{-\psi R_{mm}}(-\psi R_{mm}(\psi R_{mm} + 2) - 2) + 2)$, $\hat{E}_3 = (e^{-\psi R_{mm}}(-\psi R_{mm}(\psi R_{mm}(\psi R_{mm} + 3) + 6) - 6) + 6)$, $\hat{E}_4 = (e^{-\psi R_{mm}}(-\psi R_{mm}(\psi R_{mm}(\psi R_{mm}(\psi R_{mm} + 4) + 12) + 24) - 24) + 24)$, $\hat{E}_5 = (e^{-\psi R_{mm}}(-\psi R_{mm}(\psi R_{mm}(\psi R_{mm}(\psi R_{mm}(\psi R_{mm} + 5) + 20) + 60) + 120) - 120) + 120)$ and $\psi = \bar{\lambda}\rho\Psi$. When the number of blockage types is greater than one $N_g > 1$, The result in (16) is reached after summing up all the probabilities of different blockage types. ■

Next we consider special cases:

Case 1: There is at least one LOS link ($N_L = 1$) The probability of at least one LOS link being available to $\mathcal{U}_0$ can be obtained from Eq. (17):

$$\mathcal{P}^u_{N_b,1} = \sum_{j=1}^{N_b} \mathcal{S}^u_j \tag{21}$$

where $\mathcal{S}^u_j = (1-\mathfrak{s}^u_1)\cdots(1-\mathfrak{s}^u_{j-1})\mathfrak{s}^u_j$ is the probability of jth set (or jth BS since each set contains one BS) being LOS. Eq. (21) can be rewritten as:

$$\mathbb{P}^u_{N_b,1} = \underbrace{\mathfrak{s}_1}_{\mathcal{S}^u_1} + \underbrace{(1-\mathfrak{s}_1)\mathfrak{s}_2}_{\mathcal{S}^u_2} + \underbrace{(1-\mathfrak{s}_1)(1-\mathfrak{s}_2)\mathfrak{s}_3}_{\mathcal{S}^u_3} + \cdots + \underbrace{(1-\mathfrak{s}_1)(1-\mathfrak{s}_2)\cdots\mathfrak{s}_{N_s}}_{\mathcal{S}^u_{N_s}} \tag{22}$$

The first term represents the probability of closest BS being LOS, the second term represents the probability of second BS being LOS when the first BS NLOS and so on. While the last term represents the probability of furthest BS being LOS when all the closer BSs are NLOS.

Case 2: There is at least two simultaneous LOS links ($N_L = 2$)
The probability of at least two simultaneous LOS links being available to $\mathcal{U}_0$ can be obtained from Eq. (17):

$$\mathbb{P}^u_{N_b,2} = \sum_{j=1}^{N_b-N_L+1} \sum_{k=j+1}^{N_b} \mathcal{S}^u_{jk} \tag{23}$$

In this case, there are $\frac{N_b(N_b-1)}{2}$ possible sets ($N_s = \frac{N_b(N_b-1)}{2}$) to provide at least two simultaneous LOS links to $\mathcal{U}_0$. Eq. (23) can be rewritten as:

$$\mathbb{P}^u_{N_b,2} = \underbrace{\mathfrak{s}_1\mathfrak{s}_2}_{\mathcal{S}^u_{12}} + \underbrace{\mathfrak{s}_1(1-\mathfrak{s}_2)\mathfrak{s}_3}_{\mathcal{S}^u_{13}} + \underbrace{\cdots\cdots\cdots\cdots}_{\mathcal{S}^u_{14}\text{ to }\mathcal{S}^u_{(N_b-2)N_b}} + \underbrace{(1-\mathfrak{s}_1)(1-\mathfrak{s}_2)\cdots\mathfrak{s}_{N_b-1}\mathfrak{s}_{N_b}}_{\mathcal{S}^u_{(N_b-1)N_b}} \tag{24}$$

where $\mathfrak{s}_1\mathfrak{s}_2\mathfrak{s}_3\cdots\mathfrak{s}_{N_s}$ are obtained in Lemma 3, the first term ($\mathcal{S}^u_{12}$) represents the probability of the closest and the second closest BSs to $\mathcal{U}_0$ being LOS and the last term ($\mathcal{S}^u_{(N_b-1)N_b}$) represents the probability of the furtherest and the second furtherest BSs to $\mathcal{U}_0$ being LOS when all the closer BSs are NLOS.

Case 3: There is at least three simultaneous LOS links ($N_L = 3$)
The probability of at least three simultaneous LOS links being available to $\mathcal{U}_0$ can be obtained from Eq. (17):

$$\mathbb{P}^u_{N_b,3} = \sum_{j=1}^{N_b-N_L+1} \sum_{k=j+1}^{N_b-N_L+2} \sum_{m=k+1}^{N_b} \mathcal{S}^c_{jkm} \tag{25}$$

In this case, there are $\frac{N_b(N_b-1)(N_b-2)}{6}$ possible sets ($N_s = \frac{N_b(N_b-1)(N_b-2)}{6}$) to provide at least three simultaneous LOS links to $\mathcal{U}_0$. Eq. (25) can be rewritten as:

$$\mathbb{P}^u_{N_b,3} = \underbrace{\mathfrak{s}_1\mathfrak{s}_2\mathfrak{s}_3}_{\mathcal{S}^u_{123}} + \underbrace{\mathfrak{s}_1\mathfrak{s}_2(1-\mathfrak{s}_3)\mathfrak{s}_4}_{\mathcal{S}^u_{124}} + \underbrace{\cdots\cdots\cdots\cdots}_{\mathcal{S}^u_{125}\text{ to }\mathcal{S}^u_{(N_{BS}-3)(N_{BS}-1)N_{BS}}} + \underbrace{(1-\mathfrak{s}_1)(1-\mathfrak{s}_2)\cdots\mathfrak{s}_{N_b-2}\mathfrak{s}_{N_b-1}\mathfrak{s}_{N_b}}_{\mathcal{S}^u_{(N_b-2)(N_b-1)N_b}} \tag{26}$$

Case 4: There is at least four simultaneous LOS links ($N_L = 4$)
The probability of at least four simultaneous LOS links being available to $\mathcal{U}_0$ can be obtained from Eq. (17):

$$\mathbb{P}^u_{N_b,4} = \sum_{j=1}^{N_b-N_L+1} \sum_{k=j+1}^{N_b-N_L+2} \sum_{m=k+1}^{N_b-N_L+3} \sum_{n=m+1}^{N_b} \mathcal{S}^u_{jkmn} \tag{27}$$

In this case, there are $\frac{N_{BS}(N_b-1)(N_b-2)(N_b-3)}{24}$ possible sets ($N_s = \frac{N_b(N_b-1)(N_b-2)(N_b-3)}{24}$) to provide at least four simultaneous LOS links to $\mathcal{U}_0$. Eq. (27) can be rewritten as:

$$\mathbb{P}^u_{N_b,4} = \underbrace{\mathfrak{s}_1\mathfrak{s}_2\mathfrak{s}_3\mathfrak{s}_4}_{\mathcal{S}^u_{1234}} + \underbrace{\mathfrak{s}_1\mathfrak{s}_2\mathfrak{s}_3(1-\mathfrak{s}_4)\mathfrak{s}_5}_{\mathcal{S}^u_{1235}} + \underbrace{\cdots\cdots\cdots}_{} + \underbrace{(1-\mathfrak{s}_1)(1-\mathfrak{s}_2)\cdots\mathfrak{s}_{N_b-3}\mathfrak{s}_{N_b-2}\mathfrak{s}_{N_b-1}\mathfrak{s}_{N_b}}_{\mathcal{S}^u_{(N_b-3)(N_b-2)(N_b-1)N_b}} \tag{28}$$

B. Correlation Assumption

In order to consider a realistic scenario, the impact of correlation among the links needs to be captured. Next, the correlation among links is taken into consideration when investigating the probability of any link being LOS. Any blockage can block one or more BSs, for instance when $\mathcal{U}_0$ is located very close to one of the blockages, up to 50% of the network

can be blocked. As a result, this blockage blocks the LOS to a number of BSs in the system when two or more BSs are located in a small angle from the $\mathcal{U}_0$'s perspective. Since the BSs are randomly distributed in the system, they are located at different angles from $\mathcal{U}_0$'s perspective. The probability of LOS being available to any BS in the area $\pi^2 R_{mm}$ is studied in the next Theorem. Before that, we address the angle blocked by any blockage in the system.

Lemma 4: When the kth link is blocked by a blockage, the angle blocked by this blockage is giving by:

$$\beta_k = \sum_{i=1}^{N_g} \Gamma_i \arctan\left(\frac{x_i - a_1}{D_1}\right) + \arctan\left(\frac{x_i + a_1}{D_1}\right) \tag{29}$$

where D_1 is the distance to $\bar{y}_1$, a_1 is the distance between $\bar{y}_1$ and the centre of the blocking blockage and $\Gamma_i = \frac{2 z_i \rho_i \prod_{n=1}^{N_g} \frac{1-e^{-\lambda_p \rho_n \pi r_{i,n}^2}}{\rho_n \pi r_{i,n}^2}}{\bar{\lambda}_k}$ is the probability of blockage being from ith type.

Proof: When $N_g = 1$, it is assumed that the blockages form cylinder shapes with h height and x radius where x is uniformly distributed in the range $[w, \sqrt{\frac{w^2}{4} + \frac{l^2}{4}}]$. This assumption is reasonable because the orientation angle is a random variable and independent of the location. The blocked angle depends on the distance to $\mathcal{U}_0$ and the dimensions of the blockages. Given that kth link is blocked by a blockage as shown in Fig. 5, the angle β_k can be obtained from:

$$\beta_k = \arctan\left(\frac{x - a_1}{D_1}\right) + \arctan\left(\frac{x + a_1}{D_1}\right) \tag{30}$$

where a_1 is randomly distributed in $[0, x]$ as explained in **Theorem 1**. D_1 is the distance between $\mathcal{U}_0$ and the first CP on $\mathcal{L}_k$ ($\bar{y}_1$) and its expected value can be found by using Eq. (12). When $N_g > 1$, this blockage can be from any type and as a result the blocked angle depends on the characteristics of that blockage. The ratio of density of ith type to total density on $\mathcal{L}_k$ can be obtained from **Theorem 1**:

$$\Gamma_i = \frac{2 z_i \rho_i \prod_{n=1}^{N_g} \frac{1-e^{-\lambda_p \rho_n \pi r_{i,n}^2}}{\rho_n \pi r_{i,n}^2}}{\bar{\lambda}_k} \tag{31}$$

The numerator represents the density of ith type on $\mathcal{L}_k$. This result can also interpreted into any blockage located on $\mathcal{L}_k$ belong to ith type. The result is reached. ■

Theorem 2: The probability of N_L BSs being LOS to $\mathcal{U}_0$ under correlation assumption can be expressed as:

$$\mathbb{P}^c_{N_b,N_L} = \sum_{j=1}^{N_b-N_L+1} \sum_{k=j+1}^{N_b-N_L+2} \cdots\cdots \sum_{m=.+1}^{N_b-1} \sum_{n=m+1}^{N_b} \mathcal{S}^c_{jk\cdots mn} \tag{32}$$

$$\begin{aligned}\mathcal{S}^c_{jk\cdots mn} = {} & (1-\mathfrak{s}_1)(1-\xi_1\mathfrak{s}_2)(1-\mathfrak{s}_3((1-\xi_1)\xi_1) + \xi_1\xi_{12})^{\cdots}\mathfrak{s}_k \\ & ((1-\xi_1)(1-\xi_1)^{\cdots}(1-\xi_1)\xi_1 + (1-\xi_1)(1-\xi_1)^{\cdots}\xi_1 \\ & \xi_{1(j-1)} {}^{+\cdots} {}+\xi_1\xi_{12}{}^{\cdots}\xi_{12\cdots(j-2)}\,\xi_{12\cdots(j-2)(i-1)})\mathfrak{s}_k\big({}^{\cdots}+ \\ & \xi_1\xi_{12}{}^{\cdots}\xi_{12\cdots(j-2)}\xi_{12\cdots(j-2)(j-1)}\big)^{\cdots}\mathfrak{s}_m\big({}^{\cdots}{+}\xi_1\xi_{12}{}^{\cdots} \\ & \xi_{12\cdots(m-2)}\,\xi_{12\cdots(m-2)(m-1)})\mathfrak{s}_n\big({}^{\cdots}{+}\xi_1\xi_{12}{}^{\cdots}\xi_{12\cdots(m-2)} \\ & \xi_{12\cdots(m-2)(m-1)}\big)\end{aligned} \tag{33}$$

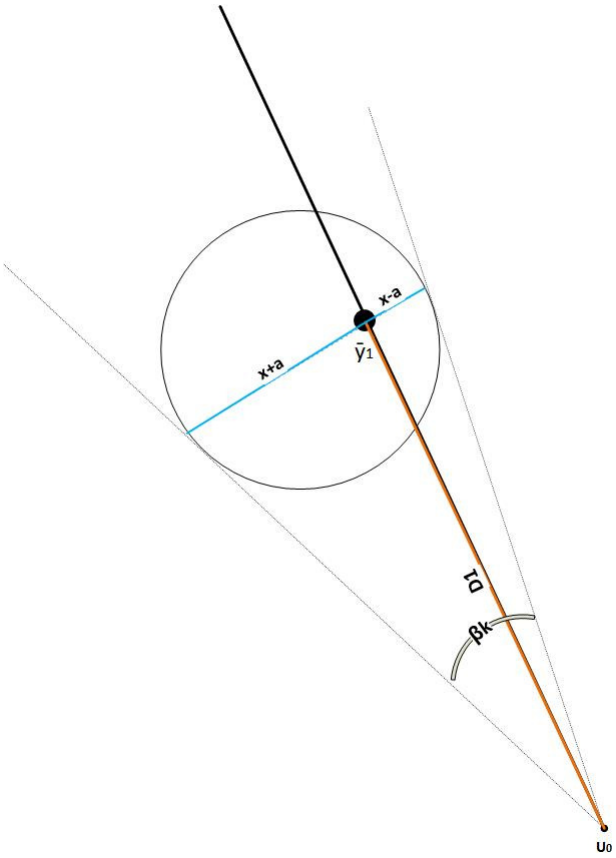

Fig. 5. Angle blocked by any blockage.

where $\mathfrak{s}_j$ is the probability of jth BS being LOS under no correlation assumption and obtained in Lemma 3, $\xi_{k,jmn} = 1 - (\frac{\beta_j+\beta_m+\beta_n}{360})$ represents the probability of kth BS being unblocked by the blockages of jth, mth and nth links.

Proof: The LOS to the kth BS is affected by whether the closer BSs are blocked or not. For instance, if the first link to $\mathcal{U}_0$ is blocked by a blockage, the 2nd link is also blocked by the same blockage if the second BS is located in the blocked angle. Therefore, the second BS is considered NLOS if a blockage located on $\mathcal{L}_2$ at distance $(R_2\Psi_i + \sqrt{r_i^2 - a_2^2})$ or this BS is located in β_1 angle. Assume that $N_b = 3$ and $N_L = 1$, the probability $\mathbb{P}^c_{3,1}$ can be expressed:

$$\begin{aligned}\mathbb{P}^c_{3,1} = {} & \underbrace{\mathfrak{s}_1}_{\mathcal{S}^c_1} + \underbrace{(1-\mathfrak{s}_1)\xi_{2,1}\mathfrak{s}_2}_{\mathcal{S}^c_2} + \\ & \underbrace{(1-\mathfrak{s}_1)(1-\xi_{2,1}\mathfrak{s}_2)\mathfrak{s}_3\big((1-\xi_{2,1})\xi_{3,1} + \xi_{2,1}\xi_{3,12}\big)}_{\mathcal{S}^c_3}\end{aligned} \tag{34}$$

where $\mathcal{S}^c_1$ represents the probability of first BS being LOS, $\mathcal{S}^c_2$ represents the probability of the second BS being LOS when the first BS is NLOS, $(1-\mathfrak{s}_1)$ represents the probability of the first BS being blocked (NLOS), $\xi_{2,1} = 1 - (\frac{\beta_1}{360})$ represents the probability of the second BS being unblocked by the same blockage of the first BS, and $\mathfrak{s}_2$ represents the probability of the second BS being unblocked by the other blockages in the system, which is obtained in Lemma 3. $\mathcal{S}^c_3$ represents the probability of the third BS being LOS when the

first and the second BSs are blocked, $(1-\xi_{2,1}\mathfrak{s}_2)$ represents the probability of the second BS being blocked, $(1-\xi_{2,1})$ represents the probability of the second BS being blocked by the same blockage of the first link, $\xi_{3,1}$ is the probability of third BS being unblocked by the blockage of the first link, $\xi_{3,12} = 1-(\frac{\beta_1+\beta_2}{360})$ represents the probability of the third BS being unblocked by the blockages of the first and second links, $(1-\xi_{2,1})\xi_{3,1}$ represents the probability of the third BS is unblocked by the blockage of the first link when this blockage blocks both the first and the second links, $\xi_{2,1}\xi_{3,12}$ represents the probability of the third BS being unblocked by any of the blockages of the first and second links when each link is blocked by different blockages. Similarly, the probability of LOS when $N_b = 4$ and $N_L = 2$ is expressed:

$$\mathbb{P}^c_{4,2} = \underbrace{\mathfrak{s}_1\mathfrak{s}_2}_{\mathcal{S}^c_{12}} + \underbrace{\mathfrak{s}_1(1-\mathfrak{s}_2)(\xi_{3,2}\mathfrak{s}_3)}_{\mathcal{S}^c_{13}} + \mathcal{S}^c_{14} + \mathcal{S}^c_{23} + \mathcal{S}^c_{24} + \mathcal{S}^c_{34} \tag{35}$$

where $\mathcal{S}^c_{14} = \mathfrak{s}_1(1-\mathfrak{s}_2)(1-\xi_{3,2}\mathfrak{s}_3)\mathfrak{s}_4((1-\xi_{3,2})\xi_{4,2}+\xi_{3,2}\xi_{4,23})$, $\mathcal{S}^c_{23} = (1-\mathfrak{s}_1)(\xi_{2,1}\mathfrak{s}_2)(\xi_{3,1}\mathfrak{s}_3)$, $\mathcal{S}^c_{24} = (1-\mathfrak{s}_1)(\xi_{2,1}\mathfrak{s}_2)(1-\xi_{3,1}\mathfrak{s}_3)\mathfrak{s}_4((1-\xi_{3,1})\xi_{4,1}+\xi_{3,1}\xi_{4,13})$ and $\mathcal{S}^c_{34} = (1-\mathfrak{s}_1)(1-\xi_{2,1}\mathfrak{s}_2)\mathfrak{s}_3((1-\xi_{2,1})\xi_{3,1}+\xi_{2,1}\xi_{3,12})\mathfrak{s}_4((1-\xi_{2,1})\xi_{4,1}+\xi_{2,1}\xi_{4,12})$ When there are N_b BSs in the system and the required number of LOS links is N_L, the results in Eq. (32) are reached. ■

Unlike the results in the previous subsection, **Theorem 2** shows that the probability of kth BS being LOS ($k \geq 2$) depends not only on the distance from this BS to $\mathcal{U}_0$ but also on the distances between the other closer BSs and $\mathcal{U}_0$.

Case 1: There is at least one LOS link ($N_L = 1$)

The probability of at least one LOS link being available to $\mathcal{U}_0$ can be obtained from Eq. (17):

$$\mathbb{P}^c_{N_b,1} = \sum_{j=1}^{N_b} \mathcal{S}^c_j \tag{36}$$

In this case, there are N_b possible sets ($N_s = N_b$) to provide at least one LOS link to $\mathcal{U}_0$. Eq. (36) can be rewritten as:

$$\mathbb{P}^c_{N_b,1} = \underbrace{\mathfrak{s}_1}_{\mathcal{S}^c_1} + \underbrace{(1-\mathfrak{s}_1)(\xi_{2,1}\mathfrak{s}_2)}_{\mathcal{S}^c_2} + \mathcal{S}^c_3 + \cdots + \mathcal{S}^c_{N_b} \tag{37}$$

where $\mathcal{S}^c_3 = (1-\mathfrak{s}_1)(1-\xi_{2,1}\mathfrak{s}_2)\mathfrak{s}_3((1-\xi_{2,1})\xi_{3,1}+\xi_{2,1}\xi_{3,12})$, $\mathcal{S}^c_{N_b} = (1-\mathfrak{s}_1)(1-\xi_{2,1}\mathfrak{s}_2)\cdots\mathfrak{s}_{N_s}((1-\xi_{2,1})\cdots\xi_{N_s,1} + \cdots + \xi_{2,1}\cdots\xi_{N_s,12\cdots(N_s-1)})$ and $\mathfrak{s}_1\mathfrak{s}_2\mathfrak{s}_3\cdots\mathfrak{s}_{N_b}$ are obtained in Lemma 3.

Case 2: There is at least two simultaneous LOS links ($N_L = 2$)

The probability of at least two simultaneous LOS links being available to $\mathcal{U}_0$ can be obtained from Eq. (17):

$$\mathbb{P}^c_{N_b,2} = \sum_{j=1}^{N_b-N_L+1} \sum_{k=j+1}^{N_b} \mathcal{S}^c_{jk} \tag{38}$$

In this case, there are $\frac{N_b(N_b-1)}{2}$ possible sets ($N_s = \frac{N_b(N_b-1)}{2}$) to provide at least two LOS links to $\mathcal{U}_0$. Eq. (38) can be rewritten as:

$$\mathbb{P}^c_{N_b,2} = \underbrace{\mathfrak{s}_1\mathfrak{s}_2}_{\mathcal{S}^c_{12}} + \underbrace{\mathfrak{s}_1(1-\mathfrak{s}_2)(\xi_{3,2}\mathfrak{s}_3)}_{\mathcal{S}^c_{13}} + \underbrace{\cdots\cdots\cdots\cdots}_{\mathcal{S}^c_{14} \text{ to } \mathcal{S}^c_{(N_b-2)N_b}} + \mathcal{S}^c_{(N_b-1)N_b} \tag{39}$$

where $\mathcal{S}^c_{(N_b-1)N_b} = (1-\mathfrak{s}_1)(1-\xi_{2,1}\mathfrak{s}_2)\cdots\mathfrak{s}_{N_b-1}\mathfrak{s}_{N_b}((1-\xi_{2,1})\cdots\xi_{N_b,1}+\cdots+\xi_{2,1}\cdots\xi_{N_b,12\cdots(N_b-2)})^2$ and $\mathfrak{s}_1\mathfrak{s}_2\mathfrak{s}_3\cdots\mathfrak{s}_{N_b}$ are obtained in Lemma 3.

Case 3: There is at least three simultaneous LOS links ($N_L = 3$)

The probability of at least three simultaneous LOS links being available to $\mathcal{U}_0$ can be obtained from Eq. (17):

$$\mathbb{P}^c_{N_b,3} = \sum_{j=1}^{N_b-N_L+1} \sum_{k=j+1}^{N_b-N_L+2} \sum_{m=k+1}^{N_b} \mathcal{S}^c_{jkm} \tag{40}$$

In this case, there are $\frac{N_b(N_b-1)(N_b-2)}{6}$ possible sets ($N_s = \frac{N_b(N_b-1)(N_b-2)}{6}$) to provide at least three simultaneous LOS links to $\mathcal{U}_0$. Eq. (40) can be rewritten as:

$$\mathbb{P}^c_{N_b,3} = \underbrace{\mathfrak{s}_1\mathfrak{s}_2\mathfrak{s}_3}_{\mathcal{S}^c_{123}} + \mathcal{S}^c_{124} + \underbrace{\cdots\cdots\cdots\cdots}_{\mathcal{S}^c_{125} \text{ to } \mathcal{S}^c_{(N_b-3)(N_b-1)N_b}} + \mathcal{S}^c_{(N_b-2)(N_b-1)N_b} \tag{41}$$

where $\mathcal{S}^c_{124} = \mathfrak{s}_1\mathfrak{s}_2(1-\mathfrak{s}_3)(\xi_{4,3}\mathfrak{s}_4)$, $\mathcal{S}^c_{(N_b-2)(N_b-1)N_b} = (1-\mathfrak{s}_1)(1-\xi_{2,1}\mathfrak{s}_2)\cdots\mathfrak{s}_{N_b-2}\mathfrak{s}_{N_b-1}\mathfrak{s}_{N_b}((1-\xi_{2,1})\cdots\xi_{N_b,1}+\cdots+\xi_{2,1}\cdots\xi_{N_b,12\cdots(N_b-2)})^3$ and $\mathfrak{s}_1\mathfrak{s}_2\mathfrak{s}_3\cdots\mathfrak{s}_{N_b}$ are obtained in Lemma 3.

Case 4: There is at least four simultaneous LOS links ($N_L = 4$)

The probability of at least four simultaneous LOS links being available to $\mathcal{U}_0$ can be obtained from Eq. (17):

$$\mathbb{P}^c_{N_b,4} = \sum_{j=1}^{N_b-N_L+1} \sum_{k=j+1}^{N_b-N_L+2} \sum_{m=k+1}^{N_b-N_L+3} \sum_{n=m+1}^{N_b} \mathcal{S}^c_{jkmn} \tag{42}$$

In this case, there are $\frac{N_b(N_b-1)(N_b-2)(N_b-3)}{24}$ possible sets ($N_s = \frac{N_b(N_b-1)(N_b-2)(N_b-3)}{24}$) to provide at least four simultaneous LOS links to $\mathcal{U}_0$. Eq. (42) can be rewritten as:

$$\mathbb{P}^c_{N_b,4} = \mathcal{S}^c_{1234} + \mathcal{S}^c_{1235} + \underbrace{\cdots\cdots\cdots\cdots}_{\mathcal{S}^c_{1236} \text{ to } \mathcal{S}^c_{(N_b-4)(N_b-2)(N_b-1)N_b}} + \mathcal{S}^c_{(N_b-3)(N_b-2)(N_b-1)N_b} \tag{43}$$

where $\mathcal{S}^c_{1234} = \mathfrak{s}_1\mathfrak{s}_2\mathfrak{s}_3\mathfrak{s}_4$, $\mathcal{S}^c_{1235} = \mathfrak{s}_1\mathfrak{s}_2\mathfrak{s}_3(1-\mathfrak{s}_4)(\xi_{5,4}\mathfrak{s}_5)$, $\mathcal{S}^c_{(N_b-3)(N_b-2)(N_b-1)N_b} = (1-\mathfrak{s}_1)(1-\xi_{2,1}\mathfrak{s}_2)\cdots\mathfrak{s}_{N_b-3}\mathfrak{s}_{N_b-2}\mathfrak{s}_{N_b-1}\mathfrak{s}_{N_b}((1-\xi_{2,1})\cdots\xi_{N_b,1}+\cdots+\xi_{2,1}\cdots\xi_{N_b,12\cdots(N_b-4)})^4$ and $\mathfrak{s}_1\mathfrak{s}_2\mathfrak{s}_3\cdots\mathfrak{s}_{N_b}$ are obtained in Lemma 3.

C. Two-Dimensional Environment

In this subsection, the 2D assumption is considered where the height of blockages, terminals and BSs are ignored. This means that any link is blocked when a blockage is located between $\mathcal{U}_0$ and the BS. Which is equivalent to a special case when $h_i \geq h_b, \forall i$. The blocking distance in Eq. (7) becomes:

$$\mathbb{B}_k = R_k \tag{44}$$

The probability of N_L links being LOS simultaneously can be obtained similar to the above scenarios:

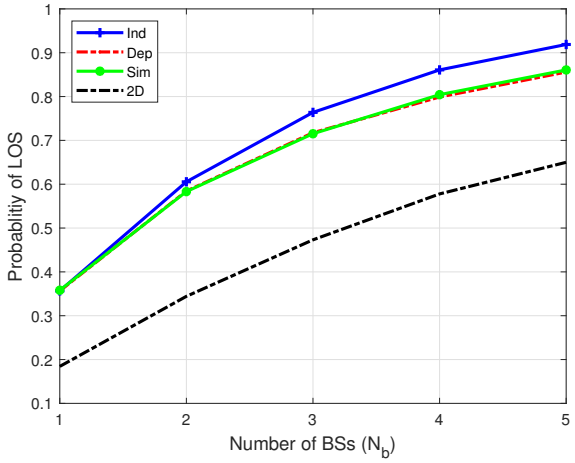

Fig. 6. Simulation vs correlated links scenario vs 2D scenario vs uncorrelated links scenario. λ_p = 1500 and N_L = 1

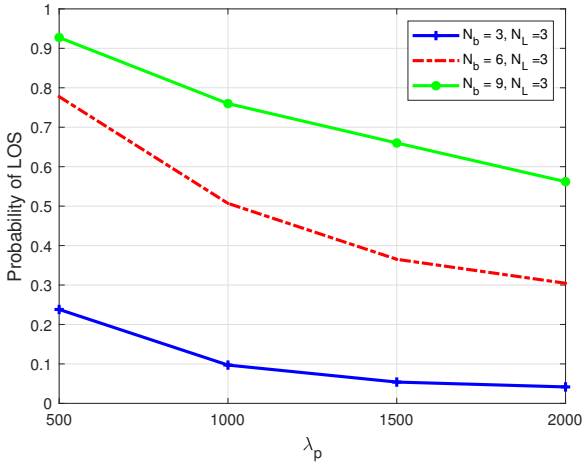

Fig. 7. Probability of LOS when N_L = 3 and N_b = 3, 6, and 9

$$\mathbb{P}^{2Do}_{N_b,N_L} = \sum_{j=1}^{N_b-N_L+1} \sum_{k=j+1}^{N_b-N_L+2} \cdots\cdots \sum_{m=.+1}^{N_b-1} \sum_{n=m+1}^{N_b} \mathcal{S}^{o}_{jk\cdots mn} \tag{45}$$

where o takes two values, c for correlated links and u for uncorrelated links. When $o = c$, $\mathcal{S}^{o}_{jk\cdots mn}$ can be obtained similar to Theorem 2:

$$\begin{aligned}\mathcal{S}^{c}_{jk\cdots mn} = {} & (1-\mathfrak{s}_1)(1-\xi_1\mathfrak{s}_2)(1-\mathfrak{s}_3((1-\xi_1)\xi_1)+\xi_1\xi_{12})^{\cdots}\mathfrak{s}_k \\ & ((1-\xi_1)(1-\xi_1)^{\cdots}(1-\xi_1)\xi_1+(1-\xi_1)(1-\xi_1)^{\cdots}\xi_1 \\ & \xi_{1(j-1)}+^{\cdots}+\xi_1\xi_{12}{}^{\cdots}\xi_{12\cdots(j-2)}\,\xi_{12\cdots(j-2)(i-1)})\mathfrak{s}_k(^{\cdots}+ \\ & \xi_1\xi_{12}{}^{\cdots}\xi_{12\cdots(j-2)}\xi_{12\cdots(j-2)(j-1)})^{\cdots}\mathfrak{s}_m(^{\cdots}+\xi_1\xi_{12}{}^{\cdots} \\ & \xi_{12\cdots(m-2)}\,\xi_{12\cdots(m-2)(m-1)})\mathfrak{s}_n(^{\cdots}+\xi_1\xi_{12}{}^{\cdots}\xi_{12\cdots(m-2)} \\ & \xi_{12\cdots(m-2)(m-1)})\end{aligned} \tag{46}$$

When $o = u$, $\mathcal{S}^{u}_{jk\cdots mn}$ becomes:

$$\mathcal{S}^{u}_{jk\cdots mn} = (1-\mathfrak{s}_1)(1-\mathfrak{s}_2)(1-\mathfrak{s}_3)^{\cdots}\mathfrak{s}_j{}^{\cdots}\mathfrak{s}_k\mathfrak{s}_m{}^{\cdots}\mathfrak{s}_n \tag{47}$$

where $\mathfrak{s}_k$ is obtained in Lemma 3 when $\mathbb{B}_k = R_k$

IV. Results

The results in this section show the accuracy of our analysis in addition to the impact of different parameters and environment's characteristics. Note that N_s = 1, R_{mm} = 200 m, l = 15 m, w = 20 m, h_u = 1.5 m, h = 20 m, h_b = 40m, λ_p = 1500 per square kilometre unless given otherwise.

Fig. 6 shows a comparison in terms of LOS availability between our analysis (considering the correlation and blockages' heights 3D), two-dimensional (2D) assumption (heights of blockages, $\mathcal{U}_0$ and BSs are ignored) similar to [13], [22] and no correlation assumption similar to [15], [17] when the number of LOS links available to $\mathcal{U}_0$ is one (N_L = 1), $h_b = 2h = 40m$ and λ_p = 1500 per square kilometre for different values of BS number (N_b). It can be seen that our analysis is very accurate. The probability of at least one BS being LOS increases when the number of BSs (N_b) increases. This is reasonable due to more potential LOS opportunities when more BSs are deployed in the system. Furthermore, deploying more BSs in the same area will result in minimizing the distances between $\mathcal{U}_0$ and BSs. The probability of LOS increases when the distances to BSs decrease because a fewer blockages are likely to be between $\mathcal{U}_0$ and the BSs. Fig. 6 also shows that the impact of correlation increases when the number of BSs in the system increases. Therefore, it is of vital importance to consider the correlation between links in a dense environment in order to obtain accurate results. For instance, the impact of correlation is very weak when the number of BSs is small (N_b = 1), while the correlation is greater when the number of BSs is higher ($N_b \geq 2$). Since the density of BSs will be very high in the future networks, ignoring the correlation among links will affect the accuracy. It is also seen that ignoring the heights of transmitters and receivers as well as the blockages can impact the results significantly due to the large difference between the blockage's height and BS's height $h_b = 2h$. However, it is anticipated that this gap is minimized when the difference between both heights is minimized.

Fig. 7 shows the probability of LOS when the ratio of number of BSs (N_b) to number of the required simultaneous LOS links (N_L) takes different values. It can be seen that the probability of LOS decreases when the blockage density increases. This is reasonable because the likelihood of blocking links in the system increases when the number of blockages increases. It can also be seen that the performance is improved when the BSs number N_b to the required simultaneous LOS links N_L ratio increases. In addition the system is more immunized against the changes in the environment when the number of BSs is high. For instance, the probability of LOS in the ratio = 1 scenario ($\frac{N_b}{N_L}$ = 1) is decreased almost six folds (from 0.24 to 0.04) when the density of blockages increases. While the reduction in the ratio = 3 scenario ($\frac{N_b}{N_L}$ = 3) is around 1.6 folds in the dense environment.

Fig. 8 and Fig. 9 capture the impact of some of the environment parameters such as the density and dimensions

This article has been accepted for publication in IEEE Transactions on Wireless Communications. This is the author's version which has not been fully edited and content may change prior to final publication. Citation information: DOI 10.1109/TWC.2023.3331657

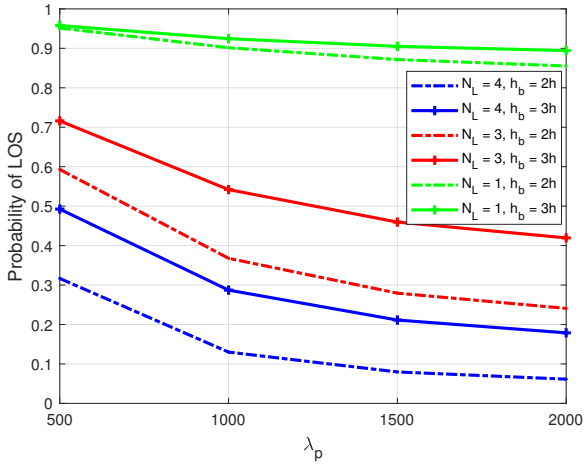

Fig. 8. Probability of LOS where $N_b = 6$, $N_L = 1, 3, 4$, $h = 15$ and, $h_b = h, 2h$ and $3h$.

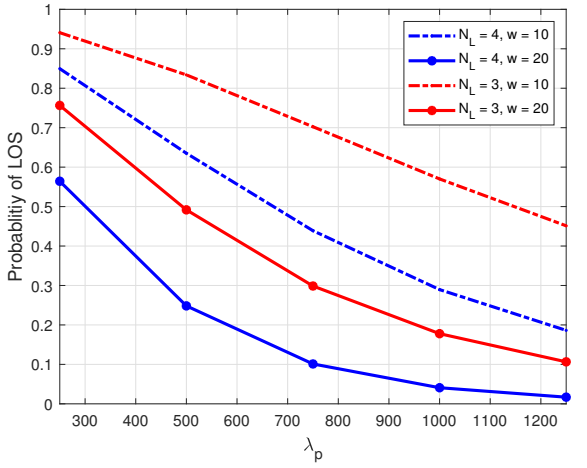

Fig. 9. Probability of LOS when $w = l = 10$ and 20, $N_b = 6$ and $N_L = 3$ and 4.

of the blockages on the availability of LOS. From Fig. 8, it can be seen that the probability of LOS is higher when the ratio of the BS height to the blockage height increases for the same number of BSs. The system performance is better when considering $h_b/h = 3$ in a very dense environment than the performance achieved when $h_b/h = 1$ in both low and high environment densities. When $h_b/h = 1$, it means any blockage will block the link to a BS if it crosses the straight line between the UE and that BS. This is considered an issue in medium and high environment densities. For instance, the probability of LOS cannot exceed 0.1 when the blockage density is high. This is not the case when $h_b/h > 1$ as some of the blockages crossing the straight line will not block the LOS to BS. Therefore, higher value of (h_b/h) can improve the system performance in different environment densities and numbers of BSs in the system. Fig. 9 shows the impact of the other parameters (e.g. width and length) on the LOS availability in the system for different values of N_L and blockage densities. It is seen from the figure that the probability of LOS decreases

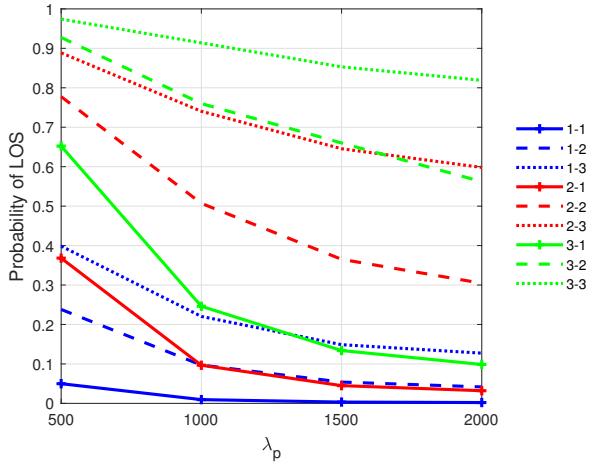

Fig. 10. Probability of LOS where $N_b = 3, 6, 9$, $N_L = 3$,$h = 20$m and $h_b = h, 2h, 3h$.

when the blockage width increases. This is reasonable as a wider blockage blocks wider scope and as a result, the likelihood of blocking a BS or more increases. Furthermore, the impact of blockage width becomes greater in more dense environments.

Fig. 10 shows LOS availability when considering 9 scenarios (different values of N_b and h_b) in different environment densities. It is assumed that $N_L = 3$ and $h = 20$ m. In the figure, $1-1$ scenario represents a scenario of $N_b/N_L = 1$ and $h_b/h = 1$, while $3-2$ scenario represents a scenario of $N_b/N_L = 3$ and $h_b/h = 2$. It can be seen from Fig. 10 that a high number of BSs provides better performance when the density of blockages is low, while higher BSs can achieve better performance in a high density environment. For example, $2-1$ scenario provides a higher LOS availability than $1-2$ scenario does when $\lambda_p < 1000$, while $1-2$ scenario provides a better LOS availability when $\lambda_p > 1000$. In addition, $3-1$ scenario is better than $1-3$ scenario when $\lambda_p < 1300$ (while $1-3$ scenario is better than $3-1$ scenario when $\lambda_p > 1300$), and $3-2$ scenario is better than $2-3$ scenario when $\lambda_p < 1600$ (while $2-3$ scenario is better than $3-2$ scenario when $\lambda_p > 1600$).

Fig. 11 and Fig. 12 show the required number of BS deployed (N_b) in the system to achieve a desired LOS availability for different values of BS heights and a different number of simultaneous LOS links required in the system when $\lambda_p = 1000$, $h = 15$ m and $h_u = 1.5$ m. The BS height is considered $h_b = 3h = 45$ m in Fig. 11 and $h_b = 2h = 30$ m in Fig. 12. From Fig. 11, it can be seen that 2 BSs $(N_b = 2)$ is required to achieve 80% availability in the system when the required number of LOS links is 1 $(N_L = 1)$. While the required number of BSs (N_b) is 5, 7 and 9 to achieve the same probability of LOS when the required number of simultaneous LOS links is 2, 3 and 4 respectively.

Fig. 12 $(h_b = 2h)$ shows that the required number of BSs N_b is 4, 7, 10 and 13 to achieve at least 80% availability when the required number of simultaneous LOS links (N_L) is 1, 2, 3 and 4 respectively. It is seen from Fig. 12 that the heights

This article has been accepted for publication in IEEE Transactions on Wireless Communications. This is the author's version which has not been fully edited and content may change prior to final publication. Citation information: DOI 10.1109/TWC.2023.3331657

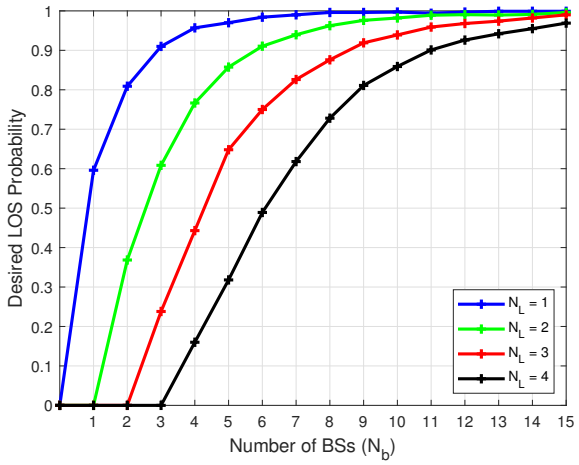

Fig. 11. Desired LOS probability. λ_p = 1500 and h_b/h = 3.

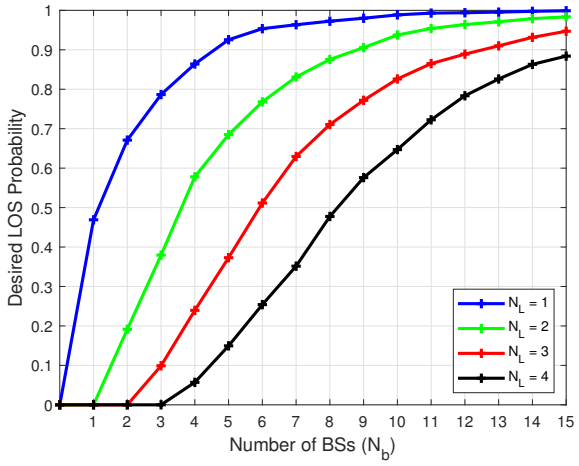

Fig. 12. Desired LOS probability. λ_p = 1500 and h_b/h = 2.

of blockages, transmitters and receivers have a great impact on the system performance and these parameters need to be taken into account in the system design.

V. Conclusion

The stochastic geometry tool was used to present a new framework in which the probability of UEs being provided with LOS was addressed by taking into consideration the blockages' characteristics and the correlation among links. The results in this paper showed the impact of the environments' characteristics (e.g. density, dimensions of the blockages) as well as the correlation among links. The results also showed that the accuracy of analysis may be affected significantly when some of the environments' characteristics (e.g height of blockages) are not considered. Ignoring the correlation between links may also cause misleading information when studying the LOS availability in dense environments and networks. Furthermore, it was shown that some network parameters (e.g number of BSs) may help achieve better system performance in low density environments, while other parameters (e.g. height of BSs) have a greater impact on the system performance in high density environments. For instance, it was shown that the deployment scenarios of a larger number of low BSs achieves better LOS availability than the deployment scenarios of a smaller number of high BSs in low and medium environment densities. However, the deployment scenarios of a smaller number of higher BSs provides better LOS availability than the deployment scenarios of a larger number of low BSs. Other results also confirmed that the height of BSs can boost the LOS availability significantly and minimize the required number of BSs to achieve a specific LOS probability in the system. For instance, the required number of BS to achieve 3-link LOS probability of 90% is minimized from 13 BSs to 9 BSs when the height of BSs rises by half. It can be concluded that studying the environment impact and different network parameters is essential to designing the localization approaches in order to achieve high accuracy and accommodate the requirements for different applications in the future communication systems.

We believe that the importance of LOS availability will be significant for newly emerged technologies, such as UAV. Expanding this work to consider more realistic scenarios in the UAV systems is of vital importance and timely. However, studying the LOS availability in the UAV systems is left as a future work due to the scope of current work (terrestrial communications).

References

[1] M. K. Bahare et al, "The 6G Architecture Landscape - European perspective" *Zenodo*, feb, 2023.

[2] B. Amjad and O. Z. Ahmed and P. I. Lazaridis and M. Hafeez and F. A. Khan and Z. D. Zaharis, "Radio SLAM: A Review on Radio-Based Simultaneous Localization and Mapping" *IEEE Access*, vol. 11, pp. 9260–9278, 2023.

[3] L. Christos and M. Adriano K. Sunwoo and L. Sangwoo and W. Lauri and F. Carlo, "A Survey of Enabling Technologies for Network Localization, Tracking, and Navigation" *IEEE Comm. Sur. and Tuto.*, vol. 20, no. 4, pp. 3607–3644, 2018.

[4] I. F. Akyildiz and J. M. Jornet and C. Han, "Terahertz band: Next frontier for wireless communications" *Phys. Comm.*, vol. 12, pp. 16–32, 2014.

[5] T. S. Rappaport et al, "Millimeter Wave Mobile Communications for 5G Cellular: It Will Work!" *IEEE Access*, vol. 1, pp. 335–349, 2013.

[6] T. S. Rappaport and Y. Xing and G. R. MacCartney and A. F. Molisch and E. Mellios and J. Zhang, "Overview of Millimeter Wave Communications for Fifth-Generation (5G) Wireless Networks—With a Focus on Propagation Models" *IEEE Tran. on Ant. and Prop.*, vol. 65, no. 12, pp. 6213–6230, 2017.

[7] N. Patwari and P. Agrawal, "NeSh: A joint shadowing model for links in a multi-hop network" *IEEE Inter. Conf. on Acoustics, Speech and Signal Processing*, pp. 2873–2876, 2008.

[8] R. Liu and C. Zhang and J. Song, "Line of Sight Component Identification and Positioning in Single Frequency Networks Under Multipath Propagation" *IEEE Tran. on Broad.*, vol. 65, no. 2, pp. 220–233, 2019.

[9] J. Zhang and J. Salmi and E. Lohan, "Analysis of Kurtosis-Based LOS/NLOS Identification Using Indoor MIMO Channel Measurement" *IEEE Tran. on Vehic. Tech.*, vol. 62, no. 6, pp. 2871–2874, 2013.

[10] W. Cui and B. Li and L. Zhang and W. Meng, "Robust Mobile Location Estimation in NLOS Environment Using GMM, IMM, and EKF" *IEEE Sys. Jour.*, vol. 13, no. 3, pp. 3490–3500, 2019.

[11] W. Wang and G. Wang and J. Zhang and Y. Li, "Robust Weighted Least Squares Method for TOA-Based Localization Under Mixed LOS/NLOS Conditions" *IEEE Comm. Let.*, vol. 21, no. 10, pp. 2226–2229, 2017.

[12] Y. Li and S. Ma and G. Yang and K. Wong, "Robust Localization for Mixed LOS/NLOS Environments With Anchor Uncertainties" *IEEE Tran. on Comm.*, vol. 68, no. 7, pp. 4507–4521, 2020.

[13] A. K. Gupta and J. G. Andrews and R. W. Heath, "Macrodiversity in Cellular Networks With Random Blockages" *IEEE Tran. on Wireless Comm.*, vol. 17, no. 2, pp. 996–1010, 2018.

[14] S. K. Gupta and V. Malik and A. K. Gupta and J. G. Andrews, "Impact of Blocking Correlation on the Performance of mmWave Cellular Networks" *IEEE Tran. on Comm.*, vol. 70, no. 7, pp. 4925–4939, 2022.

[15] C. Galiotto and N. K. Pratas and N. Marchetti and L. Doyle, "A stochastic geometry framework for LOS/NLOS propagation in dense small cell networks" *IEEE Inter. Confer. on Comm. (ICC)*, pp. 2851–2856, 2015.

[16] J. G. Andrews and T. Bai and M. N. Kulkarni and A. Alkhateeb and A. K. Gupta and R. W. Heath, "Modeling and Analyzing Millimeter Wave Cellular Systems" *IEEE Tran. on Comm.*, vol. 65, no. 1, pp. 403–430, 2017.

[17] T. Bai and R. Vaze and R. W. Heath, "Analysis of Blockage Effects on Urban Cellular Networks" *IEEE Tran. on Wireless Comm.*, vol. 13, pp. 5070–5083, Sep. 2014.

[18] K. Han and K. Huang and R. W. Heath, "Connectivity and Blockage Effects in Millimeter-Wave Air-To-Everything Networks" *IEEE Wireless Comm. Let.*, vol. 8, no. 2, pp. 388–391, 2019.

[19] T. Bai and R. W. Heath, "Coverage and Rate Analysis for Millimeter-Wave Cellular Networks" *IEEE Tran. on Wireless Comm.*, vol. 14, no. 2, pp. 1100–1114, 2015.

[20] S. Singh and M. N. Kulkarni and A. Ghosh and J. G. Andrews, "Tractable Model for Rate in Self-Backhauled Millimeter Wave Cellular Networks" *IEEE Jour. on Selec. Areas in Comm.*, vol. 33, pp. 2196–2211, Oct. 2015.

[21] M. Di Renzo and W. Lu and P. Guan, "The Intensity Matching Approach: A Tractable Stochastic Geometry Approximation to System-Level Analysis of Cellular Networks" *IEEE Tran. on Wireless Comm.*, vol. 15, no. 9, pp. 5963–5983, 2016.

[22] S. Aditya and H. S. Dhillon and A. F. Molisch and H. M. Behairy, "A Tractable Analysis of the Blind Spot Probability in Localization Networks Under Correlated Blocking" *IEEE Tran. on Wireless Comm.*, vol. 17, no. 12, pp. 8150–8164, 2018.

[23] D. Moltchanov and E. Sopin and V. Begishev and A. Samuylov and Y. Koucheryavy and K. Samouylov, "A Tutorial on Mathematical Modeling of 5G/6G Millimeter Wave and Terahertz Cellular Systems" *IEEE Comm. Surv. and Tuto.*, vol. 24, no. 2, pp. 1072–1116, 2022.

[24] S. Srinivasa and M. Haenggi, "Distance Distributions in Finite Uniformly Random Networks: Theory and Applications" *IEEE Tran. on Veh. Techn.*, vol. 59, no. 2, pp. 940–949, 2010.

[25] J. Guo and S. Durrani and X. Zhou, "Outage Probability in Arbitrarily-Shaped Finite Wireless Networks" *IEEE Tran. on Comm.*, vol. 62, no. 2, pp. 699–712, 2014.

[26] D. Stoyan and W. S. Kendall and J. Mecke, *Stochastic Geometry and Its Applications*. John Wiley and Sons Ltd., 1995.

[27] M. Gapeyenko and D. Moltchanov and S. Andreev and R. W. Heath, "Line-of-Sight Probability for mmWave-Based UAV Communications in 3D Urban Grid Deployments" *IEEE Tran. on Wireless Comm.*, vol. 20, no. 10, pp. 6566–6579, 2021.

[28] X. Wang and M. C. Gursoy, "Coverage Analysis for Energy-Harvesting UAV-Assisted mmWave Cellular Networks" *IEEE Journal on Sel. Areas in Comm.*, vol. 37, no. 12, pp. 2832–2850, 2019.

[29] Y. Qin and M. A. Kishk and M. Alouini, "On the Uplink SINR Meta Distribution of UAV-Assisted Wireless Networks" *IEEE Wireless Comm. Lett.*, vol. 12, no. 4, pp. 684–688, 2023.

[30] B. Hu and L. Wang and S. Chen and J. Cui and L. Chen, "An Uplink Throughput Optimization Scheme for UAV-Enabled Urban Emergency Communications" *IEEE Internet of Things Journal*, vol. 9, no. 6, pp. 4291–4302, 2022.

[31] D. Alkama and M. A. Ouamri and M. S. Alzaidi and R. N. Shaw and M. Azni and S. M. Ghoneim, "Downlink Performance Analysis in MIMO UAV-Cellular Communication With LOS/NLOS Propagation Under 3D Beamforming" *IEEE Access*, vol. 10, pp. 6650–6659, 2022.

[32] X. Liu and Y. Liu and Y. Chen and L. Hanzo, "Trajectory Design and Power Control for Multi-UAV Assisted Wireless Networks: A Machine Learning Approach" *IEEE Tran. on Veh. Techn.*, vol. 68, no. 8, pp. 7957–7969, 2019.

[33] M. Mozaffari and W. Saad and M. Bennis and M. Debbah, "Wireless Communication Using Unmanned Aerial Vehicles (UAVs): Optimal Transport Theory for Hover Time Optimization" *IEEE Tran. on Wireless Comm.*, vol. 16, no. 12, pp. 8052–8066, 2017.

[34] A. Sonny and S. R. Yeduri and L. R. Cenkeramaddi, "Autonomous UAV Path Planning Using Modified PSO for UAV-Assisted Wireless Networks" *IEEE Access*, vol. 11, pp. 70353–70367, 2023.

[35] J. Peng and W. Tang and H. Zhang, "Directional Antennas Modeling and Coverage Analysis of UAV-Assisted Networks" *IEEE Wireless Comm. Let.*, vol. 11, no. 10, pp. 2175–2179, 2022.

[36] A. Al-Hourani and S. Kandeepan and S. Lardner, "Optimal LAP Altitude for Maximum Coverage" *IEEE Wireless Comm. Let.*, vol. 3, no. 6, pp. 569–572, 2014.